Inorg. Chem. **2008**, *47*, 7202−7206

Inorganic Chemistry
Article

Magnetic Susceptibility and Ground-State Zero-Field Splitting in High-Spin Mononuclear Manganese(III) of Inverted N-Methylated Porphyrin Complexes: Mn(2-NCH$_3$NCTPP)Br[#]

Sheng-Wei Hung,[†] Fuh-An Yang,[†] Jyh-Horung Chen,*[,†] Shin-Shin Wang,[‡] and Jo-Yu Tung*[,§]

Department of Chemistry, National Chung-Hsing University, Taichung 40227, Taiwan, Material Chemical Laboratories, Hsin-Chu 300, Taiwan, and Department of Occupational Safety and Health, Chung Hwai University of Medical Technology, Tainan 717, Taiwan

Received March 20, 2008

The crystal structures of diamagnetic dichloro(2-aza-2-methyl-5,10,15,20-tetraphenyl-21-carbaporphyrinato-N,N′,N″)-tin(IV) methanol solvate [Sn(2-NCH$_3$NCTPP)Cl$_2$·2(0.2MeOH); **6**·2(0.2MeOH)] and paramagnetic bromo(2-aza-2-methyl-5,10,15,20-tetraphenyl-21-carbaporphyrinato-N,N′,N″)-manganese(III) [Mn(2-NCH$_3$NCTPP)Br; **5**] were determined. The coordination sphere around Sn^{4+} in **6**·2(0.2MeOH) is described as six-coordinate octahedron (*OC-6*) in which the apical site is occupied by two transoid Cl^- ligands, whereas for the Mn^{3+} ion in **5**, it is a five-coordinate square pyramid (*SPY-5*) in which the unidentate Br^- ligand occupies the axial site. The *g* value of 9.19 (or 10.4) measured from the parallel polarization (or perpendicular polarization) of X-band EPR spectra at 4 K is consistent with a high spin mononuclear manganese(III) ($S = 2$) in **5**. The magnitude of axial (D) and rhombic (E) zero-field splitting (ZFS) for the mononuclear Mn(III) in **5** were determined approximately as -2.4 cm^{-1} and -0.0013 cm^{-1}, respectively, by paramagnetic susceptibility measurements and conventional EPR spectroscopy. Owing to weak C(45)−H(45A)···Br(1) hydrogen bonds, the mononuclear Mn(III) neutral molecules of **5** are arranged in a one-dimensional network. A weak Mn(III)···Mn(III) ferromagnetic interaction ($J = 0.56$ cm^{-1}) operates via a [Mn(1)−C(2)−C(1)−N(4)−C(45)−H(45A)···Br(1)−Mn(1)] superexchange pathway in complex **5**.

Introduction

In general, Electron Paramagnetic Resonance (EPR) spectroscopy at conventional microwave frequencies [X-band, ∼9 GHz (0.3 cm^{-1}); Q-band, ∼35 GHz (1.2 cm^{-1})] is not applicable to "EPR-silent" systems with integral-spin ground states where the zero-field splitting (ZFS) is larger than the microwave quantum, in particular, where the ZFS interaction approaches axial symmetry.[1−3] Thus, conventional EPR studies of high-spin manganese(III) (d^4, $S = 2$) compounds are rather limited especially for the N-confused porphyrin (NCP) complex (NCP is also known as inverted porphyrin or 2-aza-21-carbaporphyrin). Recently, essential progress has been observed in the literature concerning the synthesis and characterization of NCP and its derivatives. Hung et al.[4] reported the X-ray structure of a five-coordinate manganese(III) complex of N-confused 5,10,15,20-tetraphenylporphyrin Mn(NCTPP)Br **(1)** (NCTPP, dianion of 5,10,15,20-tetraphenyl-*N*-confused porphyrin) and Harvey and Ziegler[5] described the structural characterization of a six-coordinate Mn(III) complex of Mn(NCTPP)(py)$_2$ **(2)**. Krzystek and co-workers[6] reported the high-frequency and -field electron paramagnetic resonance (HFEPR) study of complex **2**. It turned out that the inversion of a single pyrrole ring of **2** greatly changes the equatorial ligand field exerted and leads to large magnitudes of both the axial and rhombic ZFS (respectively, $D = -3.08$ cm^{-1}, $E = -0.61$ cm^{-1}), which are unprecedented in other Mn(III) porphyrinoids.[6]

* To whom correspondence should be addressed. E-mail: jyhhchen@dragon.nchu.edu.tw (J.H.C.), joyuting@mail.hwai.edu.tw (J.Y.T.).

[#] Dedicated to Prof. Rob Dunbar (Case Western Reserve University) on the occasion of his 65th birthday.

[†] National Chung-Hsing University.
[‡] Material Chemical Laboratories.
[§] Chung Hwai University of Medical Technology.

(1) Dexheimer, S. L.; Gohdes, J. W.; Chan, M. K.; Hagen, K. S.; Armstreng, W. H.; Klein, M. P. *J. Am. Chem. Soc.* **1989**, *111*, 8923.
(2) Talsi, E. P; Bryliakov, K. P. *Mendeleev Commun.* **2004**, 111.
(3) Bryliakov, K. P.; Bahushkin, D. E.; Talsi, E. P. *Mendeleev Commun.* **1999**, 29.
(4) Bohle, D. S.; Chen, W. C.; Hung, C. H. *Inorg. Chem.* **2002**, *41*, 3334.
(5) Harvey, J. D.; Ziegler, C. J. *Chem. Commun.* **2003**, 2890.
(6) Harvey, J. D.; Ziegler, C. J.; Telser, J.; Ozarowski, A.; Krzystek, J. *Inorg. Chem.* **2005**, *44*, 4451.

10.1021/ic800490t CCC: $40.75
Published on Web 07/23/2008

Recently, Ziegler et al.[7] reported an improved methodology for the synthesis of 2-N-methyl-5,10,15,20-tetraphenyl-21-carbaporphyrin, 2-NCH_3NCTPPH **(3)**. Compound **3** in this work was prepared in the way described by the Ziegler group using CH_3I and *p*-xylene in 48.6% yield. Unlike the NH tautomerism that exists in $NCTPPH_2$ **(4)**,[8] the free base **3** has only one stable form. Thus, a placement of a Mn(III) ion ($I = 5/2$) with a paramagnetism and a Sn(IV) ion ($I = 1/2$) with a diamagnetism in a core of N-methylated carbaporphyrin provides a promising route to synthesize a paramagnetic complex, bromo(2-aza-2-methyl-5,10,15,20-tetraphenyl-21-carbaporphyrinato-N,N′,N″)-manganese(II) [Mn(2-NCH_3NCTPP)Br; **5**] and a diamagnetic complex, dichloro(2-aza-2-methyl-5,10,15,20-tetraphenyl-21-carbaporphyrinato-N,N′,N″)-tin(IV) [Sn(2-NCH_3NCTPP)Cl_2; **6**]. This new diamagnetic compound **6** is used as a diamagnetic correction for **5** in the solid-state magnetic susceptibility measurements.[9] In this paper we focus on details of the manganese(III) electronic structure. Studies of temperature dependence of the magnetic susceptibility and of the effective moment show that $S = 2$ is the ground state for high-spin mononuclear Mn^{3+} in **5** at 20 °C. Application of the Bleaney−Bowers[10] equation permits evaluation of D, $|2J|$, and an average g value for powder samples. Measurement of the ESR spectrum arising from **5** with the $S = 2$ state and application of the spin Hamiltonian (eq 1) permits derivation of the rhombic ZFS parameter E.

Experimental Section

Preparation of Complex 2-NCH_3NCTPP (3). A solution of $NCTPPH_2$ **(4)** (0.5 g, 0.81 mmol) and CH_3I (0.3 mL, 2.1 mmol) in dry *p*-xylene (10 mL) in the presence of dry Cs_2CO_3 (0.5 g, 1.5 mmol) was heated for 2 h. After cooling down to room temperature (rt), the mixture was filtered and purified by column chromatographic separation with EtOAc−CH_2Cl_2 [1:4 (v/v)] as a green band on silica gel (70-230 mesh, 60 g). Further recrystallization from CH_2Cl_2−MeOH [1:2 (v/v)] afforded **3** (0.3 g, 0.47 mmol, 48.6%) as a blue solid.

Sn(2-NCH_3NCTPP)Cl_2 (6). A mixture of 2-NCH_3NCTPPH **(3)** (50 mg, 0.08 mmol) and $SnCl_2$ (300 mg, 1.6 mmol) was refluxed in pyridine (10 mL) for 30 min, poured into hexane (50 mL), and filtered, and the solid was dissolved in CH_2Cl_2. The resulting CH_2Cl_2 solution was rotary evaporated to dryness, and the residue was purified by a silica gel column using CH_2Cl_2/MeOH (2% MeOH) as the eluent, which on further recrystallization from CH_2Cl_2/MeOH afforded **6** (40 mg, 0.053 mmol, 66%) as a blue solid. Compound **6** was redissolved in CH_2Cl_2 and layered with MeOH to afford blue crystals for single-crystal X-ray analysis. ^{1}H NMR (599.95 MHz, $CDCl_3$, 20 °C): δ 8.98 [d, H_β, ^3J(H−H) = 5.4 Hz]; 8.95 [d, H_β, ^3J(H−H) = 4.8 Hz]; 8.86 [d, H_β, ^3J(H−H) = 4.8 Hz]; 8.82 [d, H_β, ^3J(H−H) = 4.2 Hz]; 8.81 [d, H_β, ^3J(H−H) = 4.2 Hz]; 8.76 [d, H_β, ^3J(H−H) = 4.2 Hz]; 8.22 [d, ^3J(H−H) = 4.2 Hz, *o*-H (*ortho* proton)] and 8.10 [d, ^3J(H−H) = 4.2 Hz, o-H]; 8.13 [d, ^3J(H−H) = 7.2 Hz, *o*-H] and 8.00 [d, ^3J(H−H) = 7.2 Hz, *o*-H]; 7.97 [d, ^3J(H−H) = 7.2 Hz, *o*-H] and 7.61 [d, ^3J(H−H) = 7.2 Hz, *o*-H]; 7.47−7.78 [m, *meta* and *para* protons]; 3.30 (s, N-CH_3). FAB-MS *m*/*z* (assignment. rel intensity): 154 ([NBA + H]$^+$, 56.82), 761 ([Sn(4-NCH_3NCTPP)]$^+$, 48.11), 796 ([Sn(4-NCH_3NCTPP)Cl]$^+$, 100). UV−vis spectrum, λ (nm) [$\varepsilon \times 10^{-3}$, M^{-1} cm^{-1}] in CH_2Cl_2: 458 (126.1), 565 (29.8), 606 (31.4), 722 (23.3), 884 (32.2).

Mn(2-NCH_3NCTPP)Br (5). A mixture of 2-NCH_3NCTPPH **(3)** (50 mg, 0.08 mmol) in CH_2Cl_2 (20 mL) and $MnBr_2$ (52 mg, 0.24 mmol) in MeOH (1 mL) was refluxed for 3 h. After concentrating it, the residue was dissolved in CH_2Cl_2 and filtered. The filtrate was concentrated and the residue was purified by a silica gel column using CH_2Cl_2/EA [20% EA (ethyl acetate)] as the eluent to yield impure **5**, which upon further recrystallization from CH_2Cl_2/EA afforded **5** (37 mg, 0.049 mmol, 61%) as a pure green solid. Compound **5** was redissolved in CH_2Cl_2 and layered with EA to afford green crystals for single-crystal X-ray analysis. FAB-MS *m*/*z* (assignment. rel intensity): 629 ([4-NCH_3NCTPP]$^+$, 27.35), 681 ([Mn(4-NCH_3NCTPP)]$^+$, 100), 762 ([Mn(4-NCH_3NCTPP)Br + H]$^+$, 4.67). UV−vis spectrum, λ (nm) [$\varepsilon \times 10^{-3}$, $M^{-1}cm^{-1}$] in CH_2Cl_2: 396 (35.9), 416 (34.1), 459 (24.6), 508 (59.3), 582 (10.7), 752 (10.1), 815 (12.7), 884 (12.3). Anal. Calcd. for $C_{45}H_{30}BrMnN_4$: C, 70.90; H, 3.90; N, 7.30. Found: C, 70.49; H, 4.17; N, 7.22.

Magnetic Susceptibility Measurements. The solid-state magnetic susceptibilities were measured under helium on a Quantum Design MPMS5 SQUID susceptometer from 2 to 300 K at a field of 5 kG. The sample was held in a Kel-F bucket. The bucket had been calibrated independently at the same field and temperature. The raw data for **5** were corrected for the molecular diamagnetism. The diamagnetic contribution of the complex **5** was measured from an analogous diamagnetic metal complex, that is, **6**. The details of the diamagnetic corrections made can be found in ref 9.

Spectroscopy. ESR spectra were measured on an X-band Bruker EMX-10 spectrometer equipped with an Oxford Instruments liquid helium cryostat. Magnetic field values were measured with a digital counter. The X-band resonator was a dual-mode cavity (Bruker ER 4116 DM). ^{1}H NMR spectra were recorded at 599.95 MHz on a Varian Unity Inova-600 spectrometer using the solvent $CDCl_3$ and $\delta = 7.24$ as the reference peak. Element analyses were carried out on an Elementar Vario EL III analyzer.

The positive-ion fast atom bombardment mass spectrum (FABMS) was obtained in a nitro benzyl alcohol (NBA) matrix using a JEOL JMS-SX/SX 102A mass spectrometer. UV−vis spectra were recorded at 20 °C on a Hitachi U-3210 spectrophotometer.

Crystallography. Table 1 presents the crystal data as well as other informations for **5** and **6**·2(0.2MeOH). Measurements were taken on a Bruker AXS SMART-1000 diffractometer using monochromatized Mo Kα radiation ($\lambda = 0.71073$ Å). Empirical absorption corrections were made for both complexes. The structures were solved by direct methods (SHELXTL-97)[11] and refined by the full-matrix least-squares method. All non-hydrogen atoms were refined with anisotropic thermal parameters, whereas all hydrogen atoms were placed in calculated positions and refined with a riding model. The Br coordination to Mn(1) within **5** is disordered with an occupancy factor of 0.6 for Br(1) and 0.4 for Br(1′). These Br(1) and Br(1′) atoms were also refined with anisotropic thermal parameters. Table 2 lists selected bond distances and angles for both complexes.

(7) Ou, W.; Ding, T.; Cetin, A.; Harvey, J. D.; Taschner, M. J.; Ziegler, C. J. *J. Org. Chem.* **2006**, *71*, 811.
(8) Chmielewski, P. J.; Latos-Grazynski, L. *J. Chem. Soc., Perkin Trans. 2* **1995**, 503.
(9) Drago, R. S. *Physical Methods for Chemists*, 2nd ed.; Saunders College Publishing: New York, 1992; pp 473−475, 591−593.
(10) Bleaney, B.; Bowers, K. D. *Proc. R. Soc. London.* **1952**, *A214*, 451.
(11) Sheldrick, G. M. *SHELXL-97. Program for Refinement of Crystal Structure from Diffraction Data*; University of Gottingen: Gottingen, Germany, 1997.
(12) Xie, Y.; Morimoto, T.; Furuta, H. *Angew. Chem., Int. Ed.* **2006**, *45*, 6907.

Table 1. Crystal Data for **5** and **6**·2(0.2MeOH)

formula	$C_{45.4}H_{30}Cl_2N_4O_{0.4}$ Sn⟨**6**·2(0.2MeOH)⟩	$C_{45}H_{30}N_4MnBr$ (**5**)
fw	827.52	761.58
space group	$P2_1/n$	$P2_1/n$
cryst syst	monoclinic	monoclinic
a, Å	10.0782(10)	10.1225(18)
b, Å	8.3363(7)	16.506(3)
c, Å	23.747(2)	21.104(4)
α, deg	90	90
β, deg	95.061(2)	90.989(3)
γ, deg	90	90
V, Å^3	1987.3(3)	3525.6(10)
Z	2	4
F_{000}	835	1552
D_{calcd}, g cm^{-3}	1.383	1.435
μ(M_o Kα), mm^{-1}	0.815	1.547
S	1.106	1.075
cryst size, mm^3	0.31 × 0.22 × 0.20	0.158 × 0.143 × 0.125
θ, deg	2.13 to 26.08	1.93 to 26.17
T, K	293(2)	293(2)
no. of reflcns measd	3944	6976
no. of reflcns obsd	3186	4555
R1[a] (%)	6.67	7.09
wR2[b] (%)	23.12	21.53

[a] $R1 = [\sum||F_o| - |F_c||/\sum|F_o|]$. [b] $wR2 = \{\sum[w(F_o^2 - F_c^2)^2]/\sum[w(F_o^2)^2]\}^{1/2}$.

Table 2. Selected Bond Distances (Å) and Angles (deg) for Compounds **5** and **6**·2(0.2MeOH)

		5	
Br(1)−Mn(1)	2.570(4)	Br(1′)-Mn(1)	2.458(7)
Mn(1)−C(2)	2.008(5)	Mn(1)−N(1)	2.051(4)
Mn(1)−N(2)	2.047(4)	Mn(1)−N(3)	2.022(4)
H(45A)−Br(1)	2.982(4)	C(45)−Br(1)	3.907(4)
C(2)−Mn(1)−N(3)	87.95(18)	N(3)−Mn(1)−N(1)	160.98(18)
C(2)−Mn(1)−N(1)	88.07(17)	C(2)−Mn(1)−N(2)	161.79(19)
N(3)−Mn(1)−N(2)	89.42(16)	N(1)−Mn(1)−N(2)	88.58(16)
C(2)−Mn(1)−Br(1′)	97.0(2)	N(3)−Mn(1)−Br(1′)	96.20(17)
N(1)−Mn(1)−Br(1′)	102.75(17)	N(2)−Mn(1)−Br(1′)	101.18(19)
C(2)−Mn(1)−Br(1)	101.99(17)	N(3)−Mn(1)−Br(1)	103.72(14)
N(1)−Mn(1)−Br(1)	95.31(14)	N(2)−Mn(1)−Br(1)	96.14(15)
C(45)−H(45A)−Br(1)	162.17(14)		
		6·2(0.2MeOH)	
Sn−C(7)	2.063(19)	Sn−Cl(1)	2.5116(17)
Sn−N(1)	2.123(5)	Sn−N(3A)	2.084(14)
Cl(1)−Sn−Cl(1A)	180.00(8)	C(7)−Sn−N(1)	91.5(5)
Cl(1)−Sn−C(7)	88.6(5)	Cl(1)−Sn−N(1)	90.55(16)
C(7)−Sn−N(3A)	172.9(7)		

Results and Discussion

Molecular Structures of 5 and 6·2(0.2MeOH). Mn(2-NCH_3NCTPP)Br **(5)** was produced in 61% yield by heating a 2-NCH_3NCTPPH **(3)** solution in CH_2Cl_2/MeOH under aerobic conditions with an excess of $MnBr_2$ (Scheme 1).

The complex Sn(2-NCH_3NCTPP)Cl_2 **(6)** was synthesized in 66% yield by reacting 2-NCH_3NCTPPH (**3**) with excess $SnCl_2$ in pyridine under aerobic conditions (Scheme 1). X-ray structures are depicted in Figure 1a for complex **5** and Figure 1b for **6**·2(0.2MeOH).

The geometry of the coordination around Mn(III) in **5** is closely related to a square-base pyramid, giving a trigonal distortion parameter (τ) value of 0.01, with Mn(III) having coordination of five, MnN_3CBr, with normal bonds to the N(1), N(2), N(3), C(2), and Br(1) atoms. The bond lengths of Mn(1)−C(2), Mn(1)−N(1), Mn(1)−N(2), Mn(1)−N(3), and Mn(1)−Br(1) in **5** are 2.008(5), 2.051(4), 2.047(4), 2.022(4), and 2.570(4) Å, respectively (Table 2).

In **6**·2(0.2MeOH), the geometry about Sn is a slightly distorted octahedron and has six-coordination with two axial

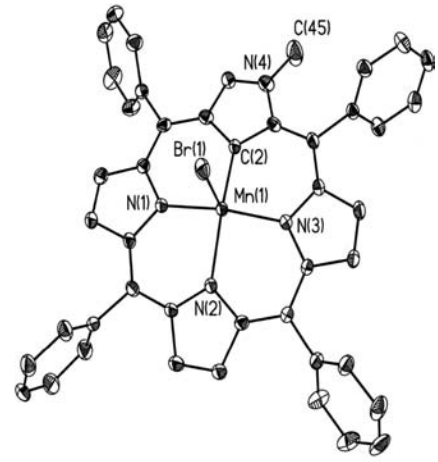

(**5**)

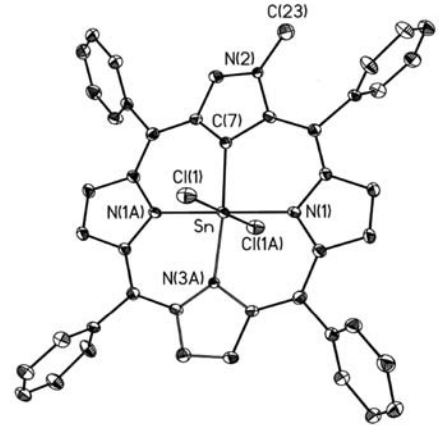

(**6**)

Figure 1. (a) Molecular structure of Mn(2-NCH_3NCTPP)Br (**5**) and (b) Sn(2-NCH_3NCTPP)Cl_2·2(0.2MeOH); **6**·2(0.2MeOH)], with 30% thermal ellipsoids. Hydrogen atoms and solvent MeOH for **6**·2(0.2MeOH)] are omitted for clarity.

Scheme 1

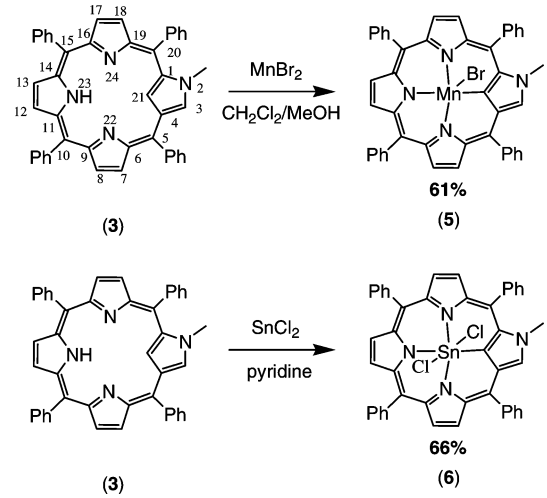

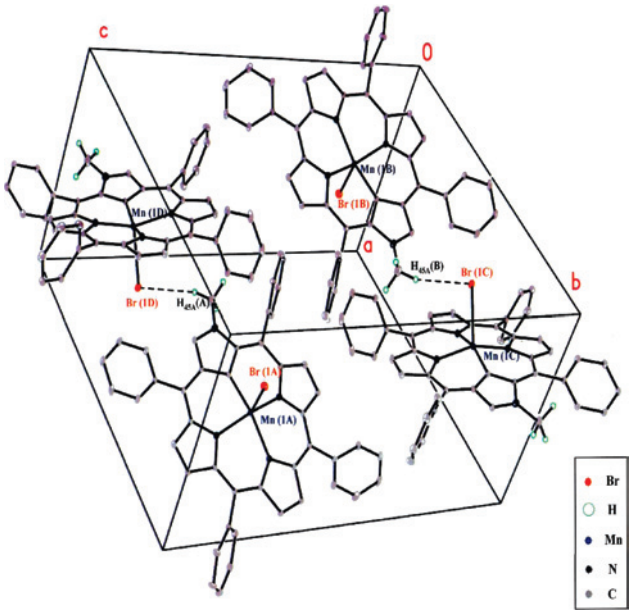

Figure 2. View of the one-dimensional network of **5** linked through weak hydrogen bonds in the unit cell.

chloride ligands; the bond distances are as follows: Sn−Cl(1) = 2.5116(17), Sn−C(7) = 2.063(19), Sn−N(1) = 2.123(5), and Sn−N(3A) = 2.084(14) Å (Table 2). The tin atom in **6**·2(0.2MeOH) is directly in the plane of the four internal core atoms, and the manganese in **5** lies 0.33 Å above the plane of the core atoms. The structure of **6**·2(0.2MeOH) is similar to that of the Sn^{4+} complex of N-confused tetraphenylporphyrin $Sn(NCTPP)Cl_2$.[12]

The crystal packing of complex **5** along the *b* axis is shown in Figure 2 in which weak hydrogen bonds link the mononuclear Mn(2-NCH_3NCTPP)Br units into an extended one-dimensional chain.

The C(45)−H(45A)···Br(1) hydrogen bond is formed mainly between C(45) and Br(1) with a C(45)···Br(1) distance of 3.907(4) Å and a corresponding angle of 162.17(14)° (Table 2). The short interatomic contacts of H(45A)···Br(1) = 2.982(4) Å provide the most likely exchange pathway (Table 2).

Spin Hamiltonian. The quintet energy levels of the high-spin mononuclear Mn^{3+} ($S = 2$) are parametrized in terms of the spin Hamiltonian[13–15]

$$(\hat{H}_s)_1 = D\left[S_z^2 - \frac{1}{3}S(S+1)\right] + E(S_x^2 - S_y^2) + \beta HgS \quad (1)$$

where H is the applied magnetic field, g is the g tensor, S is the electronic spin, and D and E are the parameters which describe the effects of the axial and rhombic ligand field, respectively. The zero-field interaction splits the levels of system with $S = 2$ spin into two doublets, one of them is a linear combination of the $m_s = |\pm 2\rangle$ states, that is, [$|2^+\rangle$, $|2^-\rangle$], and the other one of the $m_s = |\pm 1\rangle$ states, that is, [$|1^+\rangle$, $|1^-\rangle$], and a singlet corresponding to the $m_s = |0\rangle$ state,that is, $|0'\rangle$.[16] The forbidden EPR transitions may be observed between the levels of the $|2^+\rangle$, $|2^-\rangle$ non-Kramer's doublet.[1,16]

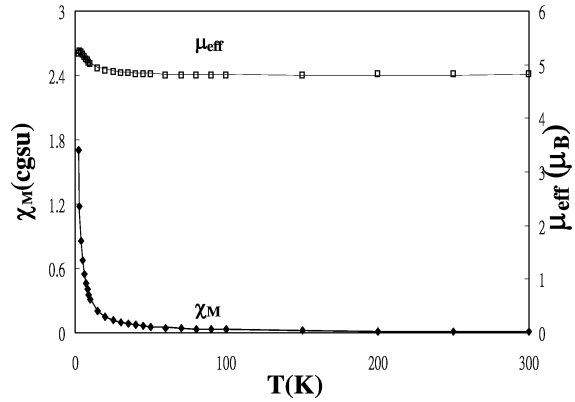

Figure 3. Temperature variation of the molar magnetic susceptibility (χ_m) and effective magnetic moment (μ_{eff}) for the powder sample of **5** in the range 2−300 K. Points represent the experimental data; solid lines represent the least-squares fit of the data to eq 2.

Magnetic Properties. Magnetic data for complex **5** are reported in Figure 3 in the forms of χ_m and μ_{eff} versus T.

As can be seen in Figure 3, the μ_{eff} for **5** remains constant at 4.83 μ_B from 300 K down to 30 K, below which it rises slowly to 5.25 μ_B at 3 K before decreasing again. This kind of behavior is expected for a high-spin mononuclear Mn(III) ($S = 2$) complex for **5** in which there is appreciable zero-field splitting of the ground state and/or weak ferromagnetic magnetic coupling. Low-symmetry $S = 5/2$ Mn(II) species, which may be present as impurities in Mn(III) compounds, can also give rise to downfield EPR signals near $g = 2$. The molecular structure of **5** shows that the metal (Mn) centers are linked by weak C(45)−H(45)···Br(1) hydrogen bonds (Figure 2), and it is known that such interactions are able to transmit interactions. From a magnetic point of view, the weak one-dimensional arrangement of **5** may then be reduced to a dinuclear one.[17] The possibility of weak magnetic exchange in **5** with the spin Hamiltonian $(\hat{H}_s)_2 = -2J\vec{S}_1\cdot\vec{S}_2 + \beta Hg_s\cdot\vec{S}_t$ for $Mn^{3+}\cdots Mn^{3+}$ dimer (with $S_1 = S_2 = 2$) is included in fitting the magnetic susceptibility data.[18] Here $\vec{S}_t$ is the total spin operator, that is, $S_t = 0, 1, 2, 3, 4$ and $g_s = (g_1 + g_2)/2$.[18] The data were inserted into the Bleaney−Bowers equation (eq 2) and the term p (or q) which is the fraction of Mn^{3+}(or $Mn^{3+}\cdots Mn^{3+}$ dimer), respectively,[19,20] where $y = 1.44D$ (cm^{-1})/T and $x = 1.44J$ (cm^{-1})/T. Here g is the average g value, TIP is the temperature independent paramagnetism, p (or q) is the fraction of Mn^{3+}(or $Mn^{3+}\cdots Mn^{3+}$ dimer), and other symbols have their standard meanings. The best fits as represented in Figure 3 gave the values of $g = 1.67$, $D = -2.4$ cm^{-1}, $2J = 1.12$ cm^{-1}, $p = 0.56$, $q = 0.29$, and a temperature independent paramagnetism value TIP

(13) Gerritsen, H. J.; Sabisky, E. S. *Phys. Rev.* **1963**, *132*, 1507.
(14) Baranowski, J.; Cukierda, T.; Jezowska-Trzebiatowska, B.; Kozlowski, H. *J. Magn. Reson.* **1979**, *33*, 585.
(15) Hendrich, M. P.; Debrunner, P. G. *Biophys. J.* **1989**, *56*, 489.
(16) The formula for Non-Kramer's doublets are shown in the Supporting Information.
(17) Costes, J. P.; Dahan, F.; Donnadieu, B.; Douton, M. J. R.; Garcia, M. I. F.; Bousseksou, A.; Tuchaguess, J. P. *Inorg. Chem.* **2004**, *43*, 2736.
(18) Yang, F. A.; Guo, C. W.; Chen, Y. J.; Chen, J. H.; Wang, S. S.; Tung, J. Y.; Hwang, L. P.; Elango, S. *Inorg. Chem.* **2007**, *46*, 578.
(19) Mathe, J.; Schinkel, C. J.; Amstel, W. A. V. *Chem. Phys. Lett.* **1975**, *33*, 528.
(20) Yates, M. L.; Arif, A. M.; Manson, J. L.; Kalm, B. A.; Barkhart, B. M.; Miller, J. S. *Inorg. Chem.* **1998**, *37*, 840.

$$\chi_M = \frac{0.3749}{T} g^2 \{ p \cdot \frac{1}{3} [\overbrace{\frac{8 + 2e^{3y} + \frac{1}{y}(-\frac{8}{3} - \frac{28}{3}e^{3y} + 12e^{4y})}{2 + 2e^{3y} + e^{4y}}}^{Mn^{3+}}] + q [\underbrace{\frac{2e^{2x} + 10e^{6x} + 28e^{12x} + 60e^{20x}}{1 + 3e^{2x} + 5e^{6x} + 7e^{12x} + 9e^{20x}}}_{Mn^{3+}\text{--- }Mn^{3+}\text{(dimer)}}] + \underbrace{(1 - p - q) \times 2.917}_{Mn^{2+}\text{(impurity)}} \} + TIP \quad \ldots(2)$$

$= 1.4 \times 10^{-4}$ cm^3/mol. The negative value of $-2J$ indicates a weak ferromagnetic nature of the spin coupling in $Mn^{3+}\cdots Mn^{3+}$(dimer). The intrachain Mn$\cdots$Mn separations of 9.558(4) Å in **5** precludes direct metal−metal bonding, so superexchange via the C(45)−H(45A)$\cdots$Br(1) hydrogen bonding in $Mn^{3+}\cdots Mn^{3+}$(dimer) must be responsible for this ferromagnetic interaction (Figure 2). The shortest interchain Mn$\cdots$Mn distance of 11.508(4) Å indicates that the interchain interactions are expected to be negligible. This ferromagnetic interaction is quite weak, that is, similar to the previous result showing that coupling of Mn(III) ions with $J = -0.2$ cm^{-1} in the complex (N-(2-hydroxybenzoyl)-N′-(2-hydroxybenzylidene)propane-1,2-diamine)-bis(methanol-O)-manganese(III), $L^6Mn(CH_3OH)_2$, through π-π stacking, although antiferromagnetic.[17]

ESR Studies. The X-band EPR spectra of a frozen solution of **5** in $CHCl_3$ at 4 K is shown in Figure 4.

The field position and shape of the observed peak signal at $g = 9.19$ (or 10.4) in parallel mode (or perpendicular mode) are close to those observed for tris(acetylacetonato)-manganese(III), $Mn(acac)_3$, and are attributed to a forbidden transition within the $|2^+\rangle$ and $|2^-\rangle$ non-Kramer's doublet (Figure 4).[1,16] The resonance field for the transition between the $\varepsilon|2^+\rangle$ and $\varepsilon|2^-\rangle$ levels at a given $h\nu$ quantum is calculated either from eq 3[13,15]

$$|\varepsilon|2^+\rangle - \varepsilon|2^-\rangle| = 2\sqrt{3}r \sin\left(\frac{\phi}{3} + 120^\circ\right) = h\nu \qquad (3)$$

where $r = [(4g^2\beta^2H^2)/3 + (16D^2)/9 + 4E^2]^{1/2}$, $\cos\phi = (-q_1H^2 - q_2)/(2r^3)$, $q_1 = (-32Dg^2\beta^2)/3$, and $q_2 = (128D^3)/27 + 16DE^2$, or from eq 4[14,16]

$$F_1H^6 + F_2H^4 + F_3H^2 + F_4 = 0 \qquad (4)$$

where $F_1 = 4p_1^3$, $F_2 = 12p_1^2p_2 + 9\,p_1^2(h\nu)^2 + 27q_1^2$, $F_3 = 12p_1p_2^2 + 18p_1p_2(h\nu)^2 + 6p_1(h\nu)^4 + 54q_1q_2$, $F_4 = 4p_2^3 + 9p_2^2(h\nu)^2 + 6p_2(h\nu)^4 + (h\nu)^6 + 27q_2^2$, $p_1 = -4g^2\beta^2$, and $p_2 = (-16D^2)/3 - 12E^2$.

The rhombic zero field parameter $E = -1.3 \times 10^{-3}$ cm^{-1} is obtained by substitution of $D = -2.4$ cm^{-1} and the field position of $g = 9.19$ ($H = 730.5$ G) into either eq 3 or eq 4. Despite the lack of a C_4 rotation axis, compound **5**, which is five-coordinate, shows relatively little rhombic ZFS. This ZFS is different from that of $Mn(NCTPP)(py)_2$ (**2**), which is six-coordinate and has a relatively large magnitude, highly rhombic ZFS: $D = -3.08$ cm^{-1}, $E = -0.61$ cm^{-1}.

Conclusions

We have investigated two new inverted N-methyl porphyrin metal complex, namely, one paramagnetic **5** and one diamagnetic **6**, and their X-ray structures are established. A technique is also reported by combining the conventional ESR spectroscopy and magnetic susceptibility measurements to evaluate the ZFS parameters (D and E) for the high-spin mononuclear Mn(III) ($S = 2$) of **5**. The complex **5** is a mononuclear complex linked through H(45A)$\cdots$Br(1) hydrogen bonds into a one-dimensional chain and displays simple weak ferromagnetism between the Mn(III) ions.

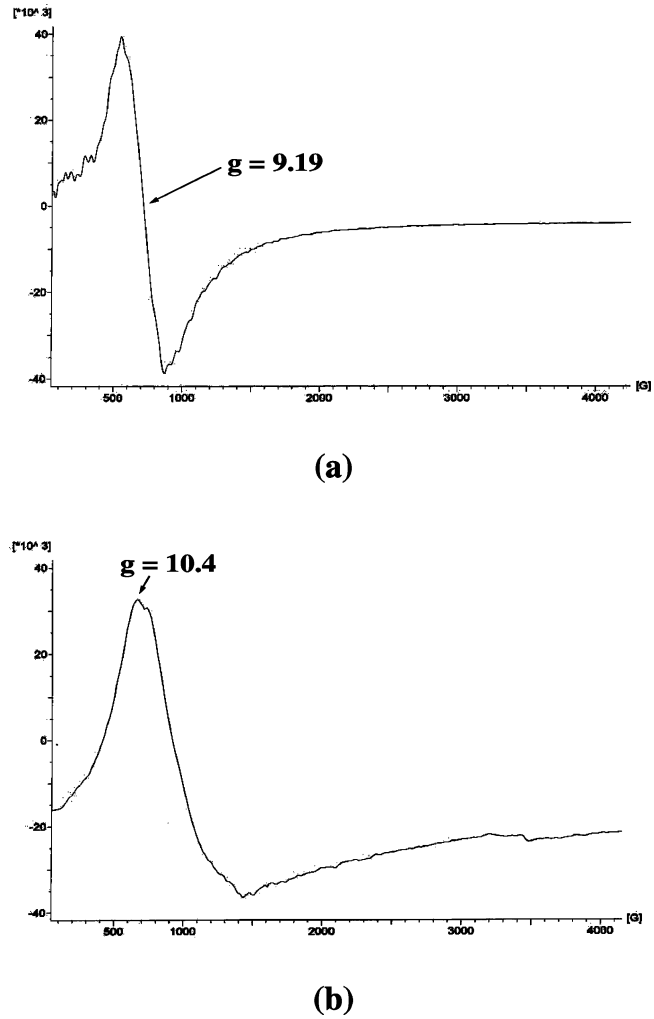

Figure 4. X-band ESR spectra for **5** in $CHCl_3$ at 4 K: (a) parallel polarization, (b) perpendicular polarization. ESR conditions: microwave frequency of 9.398 GHz (parallel polarization), 9.650 GHz (perpendicular polarization); microwave power of 3.994 mW, magnetic field modulation amplitude of 1.60 G, and modulation frequency of 100.00 KHz.

Acknowledgment. The financial support from the National Science Council of the ROC under Grant NSC 95-2113-M-005-014-MY3 is gratefully acknowledged. We thank Dr. S. Elango for helpful discussions.

Supporting Information Available: The formula for non-Kramer's doublets, ORTEP drawings with the atom-labeling schemes for complexes **5** and **6**·2(0.2MeOH) (30% probability ellipsoids), and SQUID magnetic susceptibility for **5** in the temperature range of 2−100 K. This material is available free of charge via the Internet at http://pubs.acs.org.

IC800490T